NONLINEAR SPRING AND SU-8 RAILS WITH SOLID LUBRICANT FOR ELECTROSTATIC ENERGY HARVESTER USING PARALLEL-PLATE ELECTRODES AND FERROELECTRIC

Tomokazu Takahashi[1]*, Masato Suzuki[1], Junki Onishi[1], Toshio Nishida[2], Yasuhiro Yoshikawa[2], Seiji Aoyagi[1]

[1]Department of Mechanical Engineering, Kansai University, Osaka, Japan
[2]ROHM Co. Ltd., Kyouto, Japan
*Presenting Author: t.taka@kansai-u.ac.jp

Abstract: This paper proposes a nonlinear spring and the SU-8 rails with a solid lubricant for the capacitive type energy harvester based on fringe electrical field change inside a trenched ferroelectric. The device generates power efficiently when the gap between a ferroelectric and electret is several 10 μm. The SU-8 rails can hold the gap and the amplitude loss is decreased using the solid lubricant. The mass which not connected with this nonlinear spring is moved at various frequency. The amplitude is limited by an initial distance between spring and mass. The mass moved using this vibration system when the experimental friction coefficient of solid lubricant was 0.17. The fabricated device using SU-8 rails with solid lubricant can be moved and the maximum displacement was 500 μm.

Keywords: nonlinear spring, SU-8 rail, solid lubricant

INTRODUCTION

An electret with high surface potential is used for several MEMS devices, such as a microphone, a micro power generator, etc [1-7]. A fluorocarbon polymer is well-known as an organic electret. CYTOP (Asahi Glass Co., Ltd.) is often used because of its high surface potential, long charge trapping time, and compatibility with MEMS process. A conventional type of micro energy harvester uses straight electrical field between overlapped facing electrodes [4, 7].

We proposed the principle of an electret energy harvesting method based on fringe electrical field change inside a trenched ferroelectric, as shown in Fig. 1 [8]. Compared to a conventional type, the benefits of using fringe electrical field are as follows: i) the amount of implanted charge is not discharged, even if the electret touches ferroelectric surface (confirmed by experiments in our laboratory), ii) the gap between mass and substrate can be narrowly set as far as the mechanical condition allows, and iii) high dielectric space between electrodes is realized (e.g., dielectric constant of bulk PZT or $BaTiO_3$ is more than 1,000), achieving enormous change in capacitance (ΔC) at narrow gap which leads to high output power. iv) Wiring is set on one side, which leads to mitigating packaging difficulty and lowering noise caused by stray capacitance.

STRUCTURE

Figure 2 shows the structure of the energy harvester using the nonlinear spring and SU-8 rail with solid lubricant. The comb-shaped CYTOP and Al electrodes are formed on a quartz substrate. The Si nonlinear spring is adhered on the quartz substrate. The trenched PZT mass is fixed on a Si frame. The SU-8 rails are formed on the quartz substrate and Si frame. The solid lubricant are sprayed on SU-8 rails.
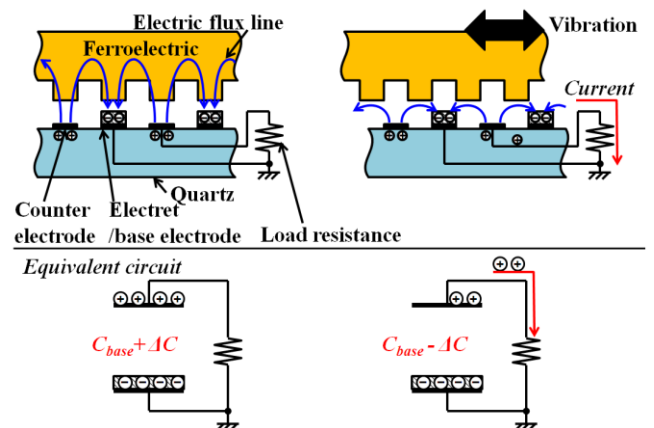

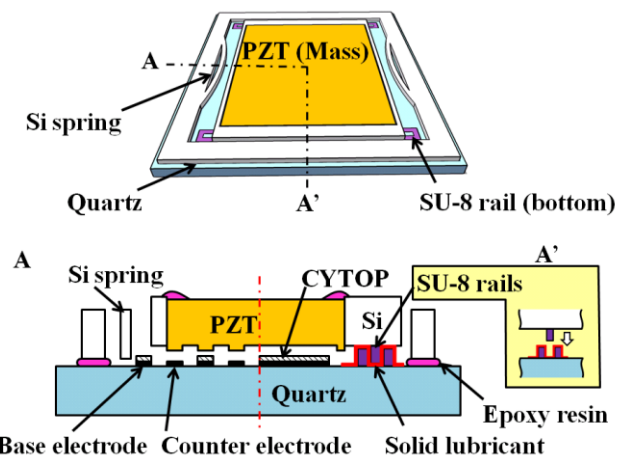Fig. 1: Proposed principle of electret energy harvesting.

Fig. 2: Schematic of structure of energy harvester using nonlinear spring and SU-8 rails with solid lubricant.

THEORY

Figure 3 shows the theoretical model of the device using the nonlinear spring and SU-8 rails with solid lubricant. This nonlinear spring The restitution force (F_{re}) of this nonlinear spring is as follow (Fig. 3(a)):

$$F_{rs} = \begin{cases} 0 & \left(|x| \le a \right) \\ k(x-a) & \left(|x| > a \right) \end{cases} \qquad (1)$$

which x, a, k are the displacement of mass, the initial gap between mass and spring, and spring constant, respectively. The input oscillation is as follow:

$$X = A\sin\omega t \qquad (2)$$

where X, A, ω are the oscillation displacement, the amplitude, and angular frequency, respectively. The applied forces are an oscillation force (F_{os}), a viscous force (F_{vi}), a friction force (F_{fr}), and an electrostatic force (F_{el}). These forces are as follow:

$$F_{os} = -A\omega^2 \sin\omega t \qquad (3)$$

$$F_{vi} = -c\dot{x} \qquad (4)$$

$$F_{os} = \mu mg\,\mathrm{sing}(\dot{x}) \qquad (5)$$

$$F_{el} = \frac{d}{dx}\left(\frac{1}{2}C_g(x)V_g(x) \right) \qquad (6)$$

where c, μ, $C_g(x)$, $V(x)$ are the viscous constant, friction coefficient, capacitance between CYTOP and ferroelectric, and the electrical potential, respectively. The dynamic equation of mass is as follow:

$$m\ddot{x} = F_{os} - F_{vi} - F_{fr} - F_{el} \qquad (7)$$

The theoretical electrical model is shown in Fig. 3(b) [2]. $C_g(x)$ is as follow:

$$C_g(t) = C_0 + \frac{\Delta C}{2}\cos\frac{2\pi}{P}x \qquad (8)$$

where C_0, ΔC, P are the base capacitance, change in capacitance in one pitch move, and the pitch of electrodes, respectively [8]. A current is as follow:

$$\frac{dQ_1}{dt} = -\frac{1}{R}\left\{ V_{el} + \left(\frac{1}{C_g(x)} + \frac{1}{C_d} \right)Q_1 \right\} \qquad (9)$$

where Q_1, R, V_{el}, C_d are the electric charge at upper electrode, the load resistance, the surface potential of CYTOP, and capacitance of CYTOP, respectively.

These formulas were calculated using the coupled numerical analysis of the Runge-Kutta method. The parameters are shown in Table 1. The oscillation amplitude and frequency were 2 mm and 10 Hz. The mass displacement was shown in Fig. 4(a) when the limited amplitude is 1 mm. The output power was in proportion to the oscillation frequency (Fig. 4(b)).
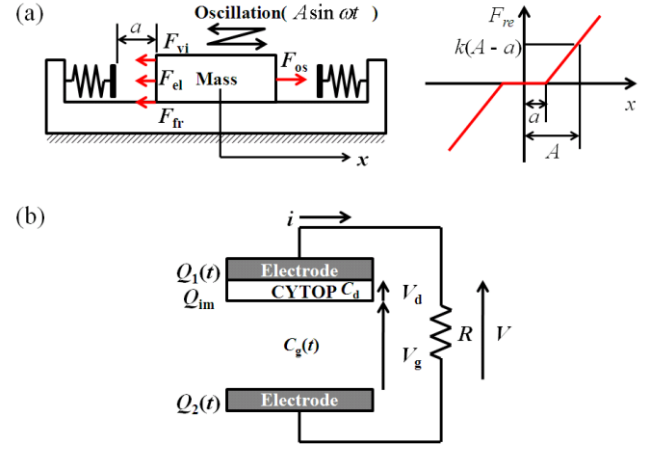

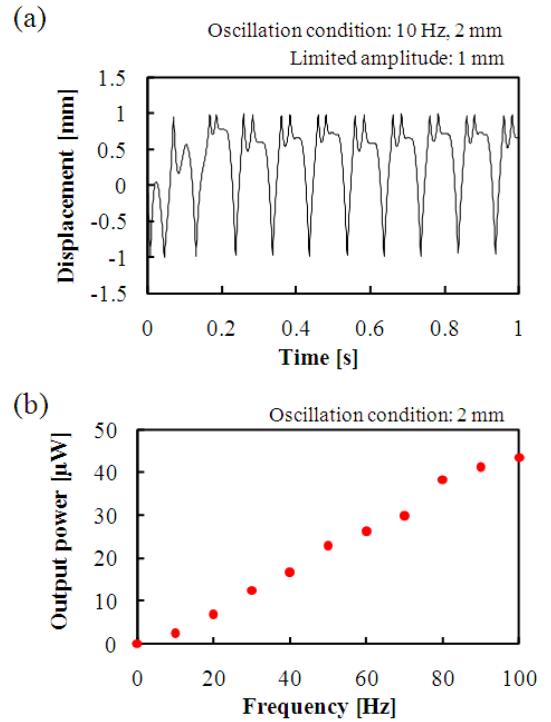Fig. 3: Schematic of (a) theoretical vibration model, and (b) electrical model.

Fig. 4: Calculation results: (a) amplitude of mass vs. time, (b) output power vs. oscillation frequency.

Table 1. Parameters of numerical analysis

Parameters	Value
A	2 mm
f	0 - 100 Hz
$r \,(= c/m\omega)$	0.1
μ	0.2
m	5 g
C_0	0.47 pF/mm^2
ΔC	0.055 pF/mm^2
P	60 μm
R	0.1 - 100 MΩ
V_{el}	−500 V
C_d	50 pF

FABRICATION

Figure 5 shows the fabrication process of the energy harvester using the nonlinear spring and SU-8 rails. This device was composed three substrate: the quartz substrate with electrodes/electret and bottom-side SU-8 rails, Si spring structure and trenched PZT with top-side SU-8 rails. The comb-shaped Al electrodes and CYTOP was patterned on the quartz substrate (Fig. 5(a)-(c)). The thickness of Al and CYTOP was 0.3μm and 5 μm, respectively. The SU-8 dry film (Nihon Kayaku Co. Ltd.,) was coated and formed into the bottom-side SU-8 rails shape. The solid lubricant sprayed on SU-8 rails using a stencil mask (Fig. 5(d)-(e)). The trench width, length and height of bottom-side SU-8 rail was 500 μm, 20 mm, 50 μm.

The Si spring and frame of PZT were fabricated by Deep RIE (Fig. 5(f)-(h)). The thickness of Si substrate was 500 μm. The trenched PZT fabricated by a dicing saw [8] is fixed on Si frame using an epoxy adhesion bond. The top-side SU-8 rails were formed on the Si frame (Fig.5 (i)-(k)). The Si spring was adhered on the quartz substrate using the epoxy adhesion bond. Finally, the PZT substrate was aligned with the quartz substrate.

EXPRIMENT

Friction coefficient

New TFE coat (Fine Chemical Japan Co. Ltd.) and Sumilon 2250 (Sumico Lubricant Co. Ltd.) were used for the solid lubricant. The main component of these lubricants is polytetrafuloroethlene (PTEF). They were sprayed on a contact surface. The friction coefficient of SU-8 rails was measured using the setup shown in Fig. 7. The coefficient of static friction was calculated based on the frequency start to move.

$$\mu = \frac{A\omega^2}{mg} \qquad (9)$$

which g is acceleration of gravity. The coefficients of static friction were shown in Table 2. The minimum coefficient was 0.17 when New TFE coat was used. Figure 8 shows the photograph of the SU-8 rails move using the high-speed camera (NAC Image Technology Co. Ltd.). The frequency and amplitude were 30 Hz and 60 μm, respectively. The amplitude of mass was 90 μm in this oscillation condition.

Table 2. Coefficient of static friction

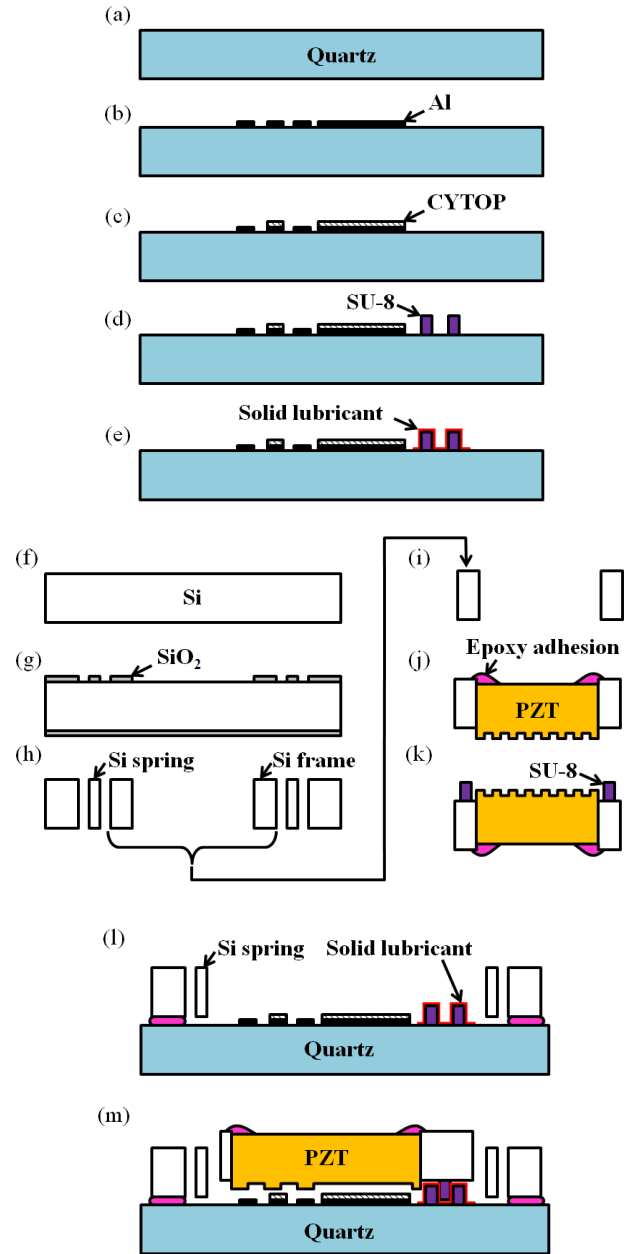| Solid lubricants	Coefficient of static friction
no coating	0.22
Sumilon 2250 (Sumico Lubricant)	0.20
New TFE coat (Fine Chemical Japan)	0.17

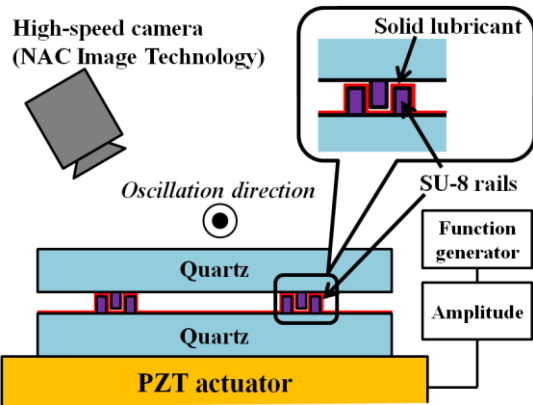*Fig. 5: Fabrication process*
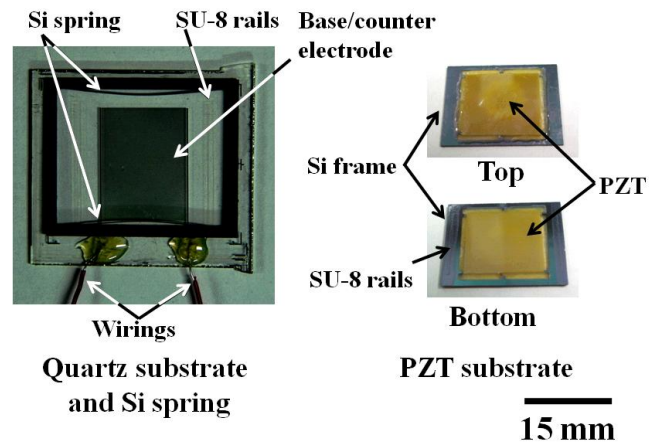
Fig. 6: Photographs of fabricated device.

Fig. 7: Schematic of setup to measure friction coefficient.

0 ms 2 ms 4 ms 6 ms 8 ms
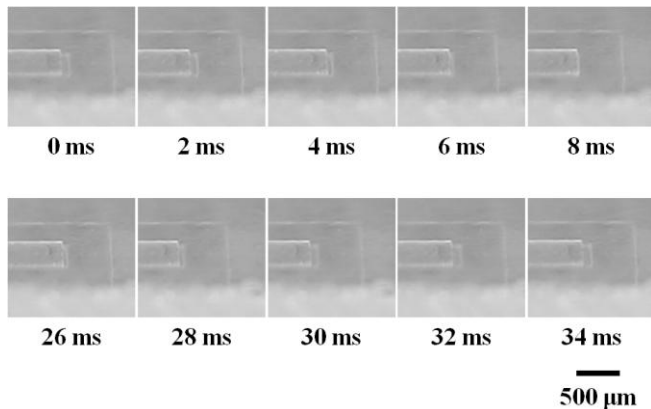
26 ms 28 ms 30 ms 32 ms 34 ms

500 µm

Fig. 8: Photographs of SU-8 rails move using High-speed camera (oscillation condition: 30 Hz, 60 µm).

Oscillation of fabricated device

Figure 9 shows the oscillation results of the fabricated device used New TFE coat for solid lubricant. The frequency and amplitude were 40 Hz and 40 µm, respectively. The PZT mass was not simple harmonic oscillation. The maximum displacement of trenched PZT mass was 500 µm.

CONCLUSION

The vibration system using the nonlinear spring is proposed. The theoretical vibration displacement and output power was calculated using the coupling numerical analysis. The mass moves between springs from the calculated results. The output power was estimated 2 µW at 10 Hz/2 mm oscillation.

The SU-8 rails were fabricated on the quartz substrates. The solid lubricants were sprayed on SU-8 rails. New TFE coat and Sumilon 2250 was used for the solid lubricant. The quartz substrates were oscillated and observed using high-speed camera. The amplitude of mass was 90 µm at 30 Hz/60 µm forced oscillation. The coefficient of static friction of New TFE coat and Sumilon 2250 were 0.17 and 0.20, respectively.

The Si nonlinear spring and the SU-8 rails was fabricated experimentally. The device using New TFE coat was oscillated in 40 Hz/40 µm. The displacement of mass was not simple harmonic vibration. The maximum displacement was 500 µm.
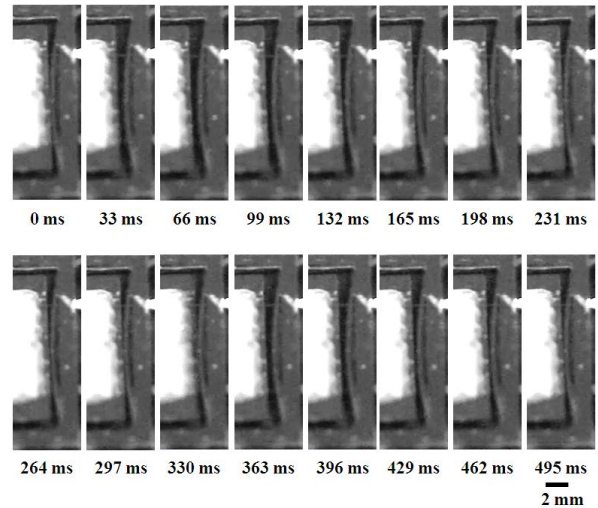

0 ms 33 ms 66 ms 99 ms 132 ms 165 ms 198 ms 231 ms

264 ms 297 ms 330 ms 363 ms 396 ms 429 ms 462 ms 495 ms

2 mm

Fig. 9: Photographs of trenched PZT mass move (oscillation condition: 40 Hz, 40 µm).

REFERENCES

[1] W. H. Hsieh, T. J. Yao, and Y. C. Tai 1999 A Micromachined Thin-film Teflon Electret Microphone, *Technical Digest Int. Conf. Solid State Sensors Actuators (Transducers '99, Sendai, Japan, 7-10 June 1999)* 1064-1067

[2] J. Boland, C. H. Chao, Y. Suzuki, and Y. C. Tai 2003 Micro electret power generator *Technical Digest MEMS 2003 (Kyoto, Japan, 19-23 January 2003)* 538-541

[3] T. Genda, S. Tanaka, and M. Esashi 2004 High Power Electret Motor and Generator on Shrouded Turbine *Technical Digest PowerMEMS 2004 (Kyoto, Japan, 28-30 November 2004)* 183-186

[4] Y. Sakane, Y. Suzuki, and N. Kasagi 2008 The development of a high-performance perfluorinated polymer electret and its application to micro power generation *J. Micromech. Microeng.* **18** 104011 (6pp)

[5] H. W. Lo and Y. C. Tai 2008 Parylene-HT-based electret rotor generator *Technical Digest MEMS 2008 (Tucson, USA, 13-17 January 2008)* 984-987

[6] M. Edamoto, Y. Suzuki, and N. Kasagi 2008 Electret-based Energy Harvesting Device with Parylene Flexible Springs *Technical Digest APCOT 2008 (Taipei, Taiwan, 22-25 June 2008)* 2B3-1 (4pp)

[7] Y. Naruse, N. Matsubara, K. Mabuchi, M. Izumi, and S. Suzuki 2009 Electrostatic micro power generation from low-frequency vibration such as human motion *J. Micromech. Microeng.* **19** 094002 (5pp)

[8] T. Takahashi, M. Suzuki, T. Hirata, N. Matsushita, R. Yoneya, J. Onishi, T. Nishida, Y. Yoshikawa, and S. Aoyagi 2011 Electret Energy Harvesting Based on Fringe Electrical Field Change inside Trenched Ferroelectric *Technical Digest MEMS 2011 (Cancun, Mexico, 23-27 January 2011)* 1305-1308